Experimental analysis of the traffic-induced-vibration on an ancient lodge

Received: 19 February 2021 | Revised: 16 September 2021 | Accepted: 12 November 2021

DOI: 10.1002/stc.2900

RESEARCH ARTICLE

WILEY

Experimental analysis of the traffic-induced-vibration on an ancient lodge

Giacomo Zini | **Michele Betti** | **Gianni Bartoli**

Department of Civil and Environmental Engineering, Università degli Studi di Firenze, Florence, Italy

Correspondence
Michele Betti, Department of Civil and Environmental Engineering, Università degli Studi di Firenze, Florence, Italy.
Email: michele.betti@unifi.it

Funding information
Municipality of Florence

Summary

Traffic-induced vibration is one of the main causes of small (often only cosmetic) damages for Heritage buildings. The heavy public road-transport, often very close to these structures, may lead to fatigue phenomena due to induced continuous vibrations and consequently damages. Even if all the International Standards agree to define the velocity—expressed in terms of Peak Particle Velocity (PPV) or Peak Particle Component Velocity (PCPV)—as reference damage indicator, a standard procedure for calculating those values starting from accelerometers data is indeed absent (or needs to be better specified). This paper—taking into account that in most cases velocities cannot be directly measured—first compares the efficiency of two of the most common employed methods: the trapezoidal rule and the long Discrete Fourier Transform. This comparison is performed discussing the experimental activity performed on the SS. Annunziata's lodge in Florence (Italy) which is particularly exposed to traffic-induced vibrations. Subsequently, a systematic analysis of the traffic-induced vibration phenomenon was performed based on (i) dynamic identification by means of accelerometers data; (ii) calculation of the velocities (PPV and PCPV); (iii) analysis of the traffic component effects; and (iv) analysis of the Structure-Soil Interaction (SSI) by using results obtained by means of Falling Weight Tests (FWT). Eventually, a comparison with the results of a previous dynamic test campaign performed in 1994 is reported, underlining a consistent increase of the traffic-induced vibrations on the lodge possibly caused by the increase of the road unevenness.

KEYWORDS

cultural heritage buildings, numerical integration, short Fourier transform (SFT), spectral analysis, traffic-induced vibrations

1 | INTRODUCTION

The effect of the traffic-induced vibrations (vehicles, subways, trams, railways, etc.) on structures is currently one of the major challenges in vibration engineering. In urban areas, vehicular traffic is among the most common sources of

ground-borne vibrations.[1–5] The induced continuous vibrations on the structure may cause small damages, but, even if only cosmetic ones, can constitute a serious threat for the European Cultural Heritage (European CH). Several factors contribute to increase the vulnerability of CH with respect to traffic-induced vibrations, such as (i) the poor level of maintenance and the pollution effects; (ii) the increasing demand of public transport in the urban areas, leading to a massive use of heavy vehicles (buses, tram, etc.); (iii) the irregularities of the road surface in the old city centers, and (iv) the proximity of such structures to heavy traffic flows.

Despite several efforts have been spent in the last decades to describe this phenomenon with analytical[6,7] and numerical predictive models,[8–10] not so many studies[11,12] contribute to establish a direct correlation with the CH building damages. However, several Authors[13,14] have observed that the continuous vibrations can significantly speed-up the deterioration process caused by other factors (i.e., several loading cycles might induce fatigue phenomena which lead to a propagation of the existing damage pattern). Consequently, CH structures built centuries ago and located in the central areas close to major traffic flows may result the most exposed structural typology to traffic-induced cosmetic damage.

Several National and International standards[15–19] provide the operative workflow to be applied for the traffic-induced vibration analysis, suggesting at the same time different safety limits for each structural typology. Nevertheless, heterogeneity of approaches highlights that some controversies continue to surround this issue, and more efforts are needed by the scientific community to deepen this topic. This paper aims at providing a contribution in this field by means of the results of an experimental activity performed on a historical lodge in Florence (Italy). The following points are examined: (i) the integration techniques that should be used to switch from accelerations to velocities; (ii) the analysis of each single vehicle-passage to identify the factors playing the major role in the vibration intensity measured on the structure; (iii) the analysis of the response factor along the structure; and (iv) the effects of the Soil-Structure-Interaction (SSI).

The paper is organized as follows. Section 2 briefly introduces the induced-vibrations phenomenon on heritage structures, together with a review of the available standards and a short summary of the scientific contributions in this field. Section 3 describes the investigated structure subjected to the traffic-induced vibrations, while Section 4 summarizes the experimental layout adopted during the dynamic campaign. Finally, Section 5 analyzes and discusses the results of the dynamic tests, including the comparison with a testing campaign performed on the same structure about 25 years ago.

2 | LITERATURE REVIEW

Vibrations induced by human activities depend on the source vibration-properties (i.e., continuous, transient, and mixed), on the field where the waves are propagating and on the structural dynamic properties. Commonly, the reference parameter used to assess the magnitude of the vibrations is the Peak Particle Velocity (PPV) measured in three orthogonal directions.

As schematically represented in Figure 1, the physics of the problem can be described as the interaction of three factors: (i) the vibration source, (ii) the SSI, and (iii) the structural typology and its current health status. The dynamic properties of each of the above factors play a specific role in the vibration content: from the source (e.g., vehicular traffic) to the receiver (the buildings, passing through the propagating field [the soil]).

Broadly speaking, the typical frequency-range of the traffic (road and rail) is very wide, between 1 and 100 Hz.[17] Several Authors[6,7] reduced that frequency-band to 8–16 Hz for the Heavy Goods Vehicles (HGV) due to the "wheel hop" mode of vibration of the vehicle's suspension. The analysis of the dynamic properties of the pavement-soil system is a complex task because the vibratory regime induced by traffic is due to the superposition of the effects of different waves (body and surface waves) propagating in a heterogeneous field.[20] Hence, the presence of irregularities at different levels (both pavement and soil) modifies the frequency content and the amplitude of the vibration source.[21] In addition,

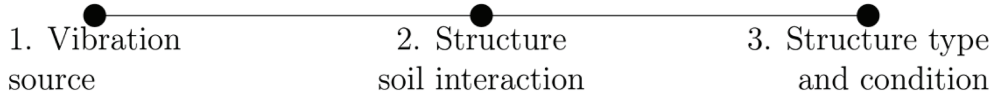

FIGURE 1 The "actors" in the induced vibration phenomenon

the resonance phenomena connected with the dynamic property of the structure alter the frequency content in the signals measured at the foundation level. These amplification phenomena might lead to severe modal strains associated with high stresses in both structural and non-structural elements. Thus, the esthetic elements (plasters, frescos, decorations, etc.) of the CH buildings, made by brittle materials with low-tensile strengths, may be proven to be the most exposed parts. The failure of these non-structural elements causes the so-called *cosmetic damage*, which can compromise not only the esthetic but also be related to serious injuries of people.

The effects of traffic-induced vibrations on buildings have been addressed by several National and International codes, and the following areas are investigated: (i) the analysis of the vibration source properties; (ii) the definition of the reference quantities for the vibration levels (and how these quantities should be measured); and (iii) the building typology and its degree of conservation. While not all the standards cover all the above topics, the PPV or the Peak Component Particle Velocity (PCPV) are univocally considered as the reference damage indexes. In the meantime, different standards establish different calculation methods to evaluate the possible damages on the structures based on the classification of the vibration-source properties. For instance, the codes define two types of vibration: short-term vibrations (or transient) and long-term vibrations (or continuous). While long-term vibrations can produce fatigue-damages connected with the structural resonance phenomena after several cycles, transient vibrations can produce damages after each application. Even though the International Standard ISO 4866:2010[17] classifies the heavy car traffic as permanent vibration, commonly the national codes give the choice to the analyst's expertise (i.e. expert judgment). Similarly, the selection of the sensors to be used for the measurements depends on the users, without any specifications on the numerical methods that should be adopted to compute the PPV. Thus, the PPV can be directly measured with velocimeters or can be indirectly calculated using numerical integration or differentiation (when displacements are measured, generally an additional device is needed to remove the displacement of the target from the one of the device).[22,23] Although several sensors (e.g., Linear Velocity Transducers and Laser Doppler Vibrometer) are nowadays available to directly measure velocities, piezoelectric accelerometers are by far the most traditional and widely used sensors.[24] In fact, being sensitive to low-amplitude vibration they are usually preferred when measuring vibrations in CH case studies.

Once the experimental layout has been set and the properties of the vibration source have been assessed, all the standards give a limitation in terms of PPV or PCPV as a function of the dominant frequency. The limit curves—which are functions of the vibration regime (transient or permanent) and of the dominant frequency—are commonly called Z-curves and are available in each standard depending on the building typology and on the properties of the vibration-source. A set of Z-curves for CH buildings is shown in Figure 2 where the dependence on the dominant frequency is clear apart from the permanent-vibration case in the DIN 4150-3:1999[16] that is fixed to 2.5 mm/s for every frequency band. The Z-curve proposed by the DIN 4150-3:1999[16] is adopted by other national codes, such as the Italian standards UNI 9916:2014.[19] Reasonably the traffic can be considered as a source of permanent vibrations. Considering that the

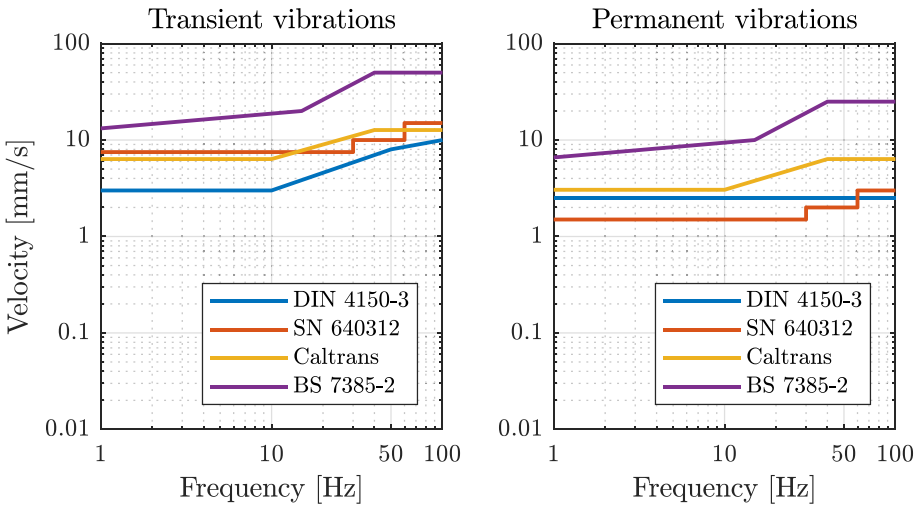

FIGURE 2 Peak Particle Component Velocity (PCPV) limits at the ground level defined by the standards: The German DIN 4150-3,[16] the Swiss SN 640312,[18] the limits proposed by Konon and Schuring[25] used by the Californian Department of Transportation (Caltrans)[26] and the British BS 7385-2:1993[15] for the CH buildings

frequency content of the vehicular traffic is approximately between 5 and 20 Hz, the limits at the ground level range from 1.5 mm/s (SN 640312:2013[18]) to 3 mm/s (as suggested by the manual used by the Californian Department of Transportation (Caltrans)[26]), up to a value of 11.5 mm/s (BS 7385-2[15]). In some studies (e.g., Domenichini et al.[27]) a lower threshold equal to 1 mm/s for the permanent vibrations to avoid damage effects in the CH buildings is proposed.

This wide range of acceptable vibration levels for CH buildings confirms that the debate is still open. Nevertheless, the problem has been studied by several researchers since the beginning of the 90's and today illustrative studies on CH structures are available as a guidance. Some of these studies are summarized in Table 1; some information can be derived from the detected damages and the measured vibration levels that are reported. However, different approaches to assess the traffic-induced vibrations magnitude have been used by the researchers. In some cases, the velocities were directly measured with velocimeters, in other cases they were indirectly calculated by integrating the measured accelerations. In previous works,[23,31] for instance, the velocities were computed from the differentiation of the displacements measured with micro-wave interferometer. However, the numerical methods used to calculate the velocities can represent a crucial point since some numerical errors can be introduced; this issue has not received much attention by the scientific community. When measuring accelerations, only few studies describe suitable techniques for the integration process to derive the velocities. For instance, Brandt et al.[36,37] suggests to use the long Discrete Fourier Transform (DFT) method, both for transient and steady-state signals, showing that the trapezoidal rule should be avoided because

TABLE 1 Experimental campaigns performed on CH buildings

Authors	Structure	First natural frequency [Hz]	Vibration source	Measurement devices	Peak values [mm/s]
Baraccani et al. (2020)[2]	Asinelli and Garisenda towers (Italy)	0.32 and 0.71	vehicular traffic	velocimeters	-
Roselli et al (2018)[28]	Temple of Minerva Medica (Italy)	2.10	vehicular. rail. tram traffic.	velocimeters	2.7[b]
Erkal (2016)[29]	Minaret of little Hagia Sophia (Turkey)	1.45	rail traffic	velocimeters	1.24[b]
Pau and Vestroni (2013)[1]	Basilica of Maxentius (Italy)	1.42	vehicular traffic	accelerometers	1–2[b]
Ma et al. (2011)[30]	Monument to the martyrs in the autumn of Xinhai Year (China)	-	metro	accelerometers	0.051[a]
Fratini et al (2011)[31]	Baptistery of San Giovanni (Italy)	2.65	vehicular traffic	micro-wave interferometer	0.06[b]
Pau and Vestroni (2008)[32]	Flavian Amphitheater (Italy)	1.03	vehicular traffic	accelerometers	-
Kliukas et al (2008)[33]	Cathedral belfry (Lithuania)	1.30	vehicular traffic	accelerometers	-
Crispino and D'Apuzzo (2001)[3]	San Teodoro palace (Italy)	-	vehicular and tram traffic	velocimeters	1.82[b]
Clemente and Rinaldis (1998)[4]	Villa Farnesina (Italy)	-	vehicular traffic	velocimeters	0.18[b]
Clemente (1995)[34]	Various monuments in Rome (Italy)	-	vehicular traffic	velocimeters and displacements transducers	0.24–2.21[b]
Chiostrini et al. (1995)[35]	Gallery of Vasari (Italy)	-	vehicular traffic	velocimeters	0.260[b]

Note: -: data not available.

[a]Peak Particle Velocity (PPV).

[b]Peak Particle Component Velocity (PCPV).

[Correction added on 13 December 2021, after first online publication: reference 29 was mistakenly added in Pau and Vestroni (2008) entry in Table 1 and has been removed in this version.]

it gives biased results, especially in the higher frequency ranges. Among the various standards, only the Italian UNI 9916:2014[19] suggests performing a time-domain integration process based on the trapezoidal rule after the application of a high-pass sixth order Butterworth filter with a cut-off frequency of 1 Hz. Even though this code also provides the selection of different values of the cutting frequency, a method is not suggested and the selection is up to the analyst's expertise.

Regarding the correlations between the vibration level and the cosmetic damages, only in previous works[4,28] severe damage levels due to the traffic vibrations have been observed. Considering the information today available in the Standards and in the literature, it is possible to underline how some further steps are needed to set up reliable methods. In this respect, it would be desirable to collect a huge number of CH test-cases in order to build a large database able to correlate the vibration level and the observed damages.

3 | THE SS ANNUNZIATA'S LODGE

The lodge of the SS. Annunziata's church in Florence (Italy) (Figure 3) is a stone-masonry historic structure with a rectangular shape (about 6×40 m) and an overall height of about 15 m. Eight stone columns with a height of about

FIGURE 3 (a) Front view of the lodge from the SS. Annunziata's place (b) the DAQ system used during the test (c) lateral view inside the lodge (d) the triaxial measuring station made up with three piezoelectric accelerometers

4.50 m sustain the vaults (Figure 4). Between the vaults and the roof there is an internal level with a height of about 3.0 m (Figure 4d).

The construction dates back to 1453 and represents a great example of the Renaissance's architecture. The original design was made by Antonio da Sangallo, even if the structure was subsequently modified between 1599 and 1604 by Giovan Battista Caccini. In recent time, around the 1930s, the lodge was strengthened with the insertion of several tie rods in the vaults, and a concrete flat slab was built substituting the wooden roof. Several restorations took place in the last decades to repair the esthetic parts (plasters, frescos, cornices, etc.).

The lodge is located in front of SS. Annunziata square that is crossed from heavy vehicular traffic running just some meters outside the church. The bus passage in front of the lodge is quite heavy, with five different bus lines that stop just in front of it. In addition, the road pavement is mainly built with fan-pattern setts and in some points with asphalt, leading to a very irregular surface. Despite the theoretical speed-limit of the vehicles (less than 50 km/h), the source of the vibrations is very close to the structure, and the road unevenness is large, leading to considerable traffic-induced vibrations. These factors play a major role in the magnitude of the traffic-induced vibrations (as also reported in the predictive traffic induced vibration models proposed by Watts[6]).

Since the environmental context of the SS. Annunziata lodge is recurrent in most of the historic city centers, the discussion of its case is very useful to clarify several points in the traffic-induced vibrations assessment on the CH buildings. In addition, the availability of a dynamic testing campaign that took place about 25 years ago allows for time comparison. A similar experimental layout was used to directly compare the results of the two experimental campaigns, assessing the variation of the vibration levels after such a long period.

4 | DYNAMIC TEST CAMPAIGNS

To assess the level of the traffic-induced vibrations and the effect of the Soil-Structure-Interaction two dynamic test campaigns were performed.

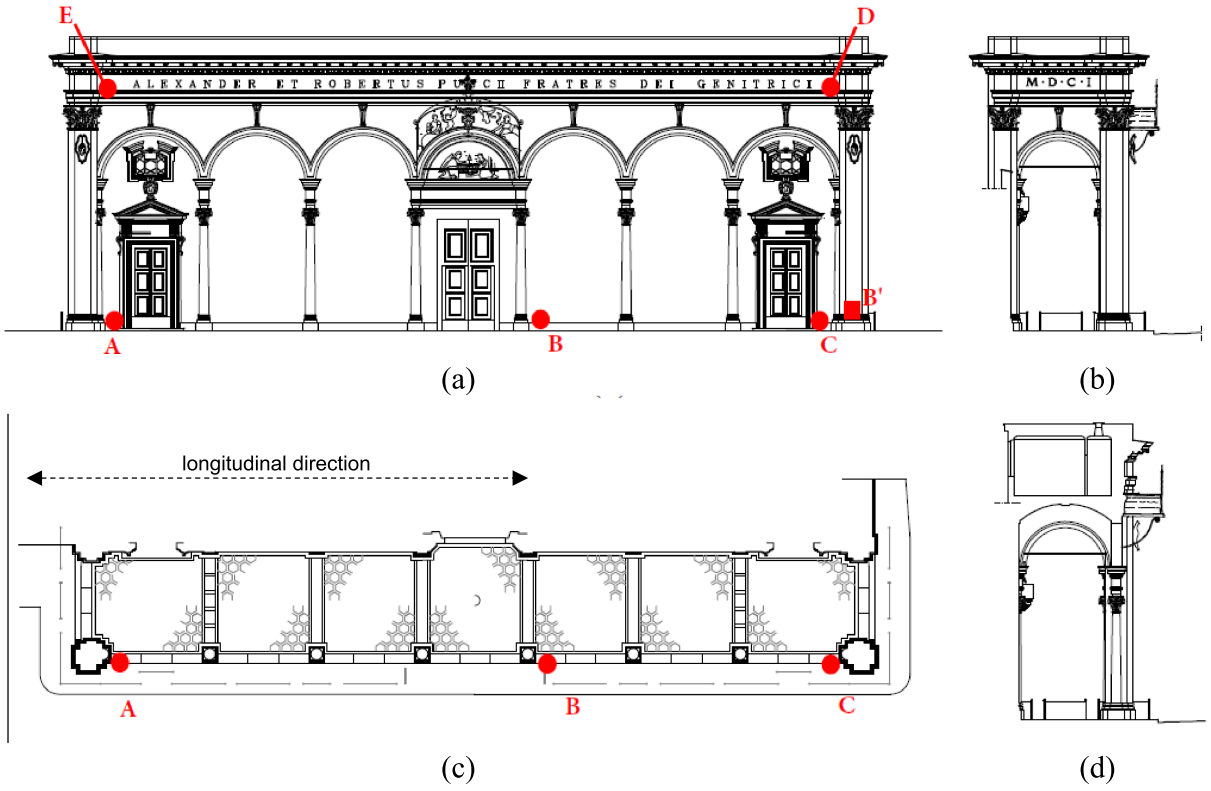

FIGURE 4 (a) Frontal view of the structure and the sensors layout for all the dynamic tests and the lateral view (b) plan of the ground level with the sensors layout (c) and the section of the lodge (d)

The first testing campaign was performed in February 2019. Five triaxial stations (denoted from A to E in Figure 4) equipped with piezoelectric accelerometers (PCB 393-B31/B12 and 393-C, respectively, with a measurement range of 0.5 and 2.5 g and a sensitivity of 10 and 1 V/g) were used to acquire an entire day of traffic. Three stations were placed at the ground level, corresponding to the corners and the middle of the structure, and two stations at the upper level as shown in Figures 4a and 4c (setup #1). To preserve the architectonical features of the structure, the stations were only fixed with steel blocks (Figure 3b–d). A webcam was additionally installed close to the Data Acquisition (DAQ) unit and it was synchronized with the measurements in order to correlate the observed events with the vibration source (car, bus, truck, etc.). In the same campaign, a second layout (setup #2) was employed to measure the vibration level from the soil to the base of the column and to the upper part of the lodge. Thus, station B was moved on the base of the column (position B′ in Figure 4a) in the left corner aligning with the measuring stations C and D. The entire column was hence monitored to have an insight of the dynamic effects of each vehicle passage.

A second dynamic test campaign was performed in June 2019 to analyze the SSI. The Department of Civil and Industrial Engineering of the University of Pisa (DICI) performed the tests with a falling-weight deflectometer (FWD) machine,[38,39] type Dynatest 8000, equipped with nine geophones measuring the deflections after the weight drop. The points to hit the road pavement correspond to a horizontal alignment in front of each station (A-B-C) at the ground level to investigate the amplification effects of the soil. During this experimental campaign, the area was closed to the vehicular traffic in order to avoid noise effects in the dynamic soil characterization.

Table 2 reports the accelerometers used in both February and June 2019 experimental campaigns, their position (A-B-C-D-E) and the measuring directions. Longitudinal direction denotes the one parallel to the long dimension of the lodge (Figure 4), transversal direction is the one orthogonal.

For the tests of February 2019 (under the traffic), all the signals length was about 30 min (data were collected with a sampling rate of 1200 Hz for a total amount of 2.160.000 samples for each record), while for the impulsive tests on the road surface (June 2019) the sampling rate was increased to 2400 Hz.

5 | RESULTS AND DISCUSSION

The experimental results of all the layouts in the two dynamic-testing campaigns described in Section 4 are here discussed, focusing on the following key-points: (i) structure dynamics, (ii) numerical integration of the accelerations, (iii) analysis of the most significant traffic events, (iv) propagation of vibration from the foundation to the upper level, (v) propagation of the vibration in the soil under the road pavement, and (vi) comparison with the vibration levels measured about 25 years ago. The next subsections will focus on these topics analyzing the experimental data collected in the lodge.

5.1 | Dynamic identification

Dynamic identification of the lodge was performed using the results obtained with stations D and E. The signals were filtered in the frequency band [0.5–20 Hz], where the structural modes are supposed to be, with a third-degree Butterworth filter. The results obtained with frequency-domain techniques (Frequency Domain Decomposition (FDD) and Average Normalized Power Spectral Density (ANPSD)) are shown in Table 3 for a single record; similar results were obtained from the other records.

TABLE 2 The sensors layout for the dynamic testing campaign

Position	Vertical direction	Longitudinal direction	Transversal direction
A	A-2 (PCB 393-C)	A-3 (PCB 393-C)	A-6 (PCB 393-C)
B	A-5 (PCB 393-C)	A-8 (PCB 393-C)	A-7 (PCB 393-C)
C	A-18 (PCB 393-B31)	A-19 (PCB 393-B31)	A-1 (PCB 393-C)
D	A-9 (PCB 393-B31)	A-16 (PCB 393-B12)	A-17 (PCB 393-B12)
E	A-10 (PCB 393-B31)	A-12 (PCB 393-B31)	A-11 (PCB 393-B31)

TABLE 3 Identified resonant frequencies

	f_1 [Hz]	f_2 [Hz]	f_3 [Hz]	f_4 [Hz]	f_5 [Hz]	f_6 [Hz]	f_7 [Hz]
FDD	3.333	3.894	4.272	4.425	4.980	5.750	6.372
ANPSD	3.369	3.875	4.279	4.443	4.956	5.713	6.396

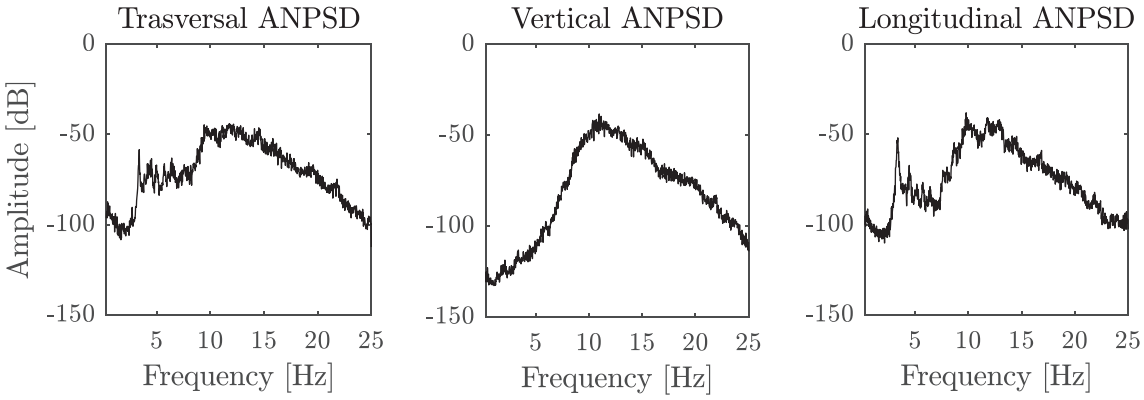

FIGURE 5 The Average Normalized Power Spectral Density (ANPSD) for each component of the measuring stations at the first floor

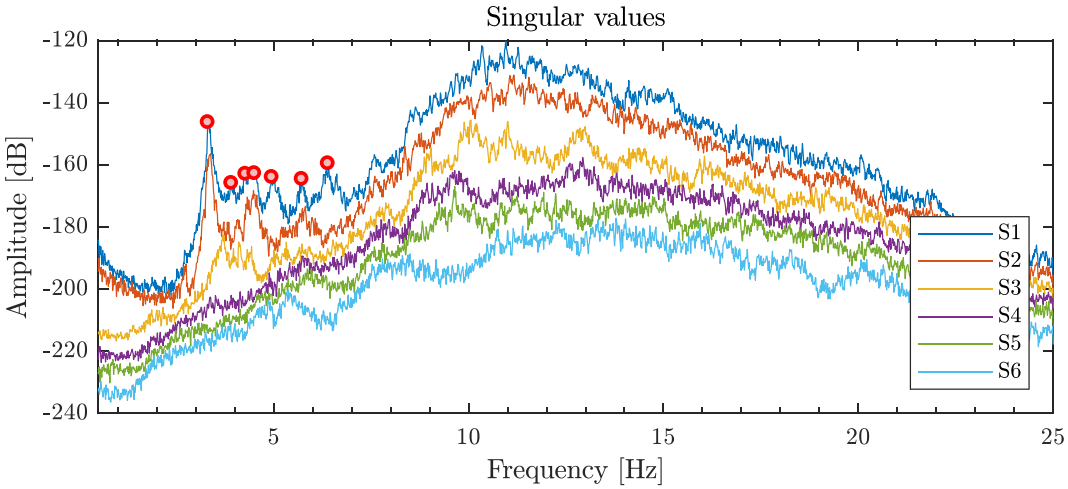

FIGURE 6 The singular value decomposition (SVD) of the power spectral density (PSD) matrix; the red circles are the identified peaks corresponding to the structural modes

The frequency content for each component is shown in Figure 5. While the frequency band from 10–20 Hz—the typical range for the vehicular traffic—exhibits the highest energy content, below 10 Hz some resonant frequencies can be identified in the longitudinal and transversal directions. In the vertical component the traffic noise is predominant, and no resonant frequencies can be clearly identified.

Similar results were obtained with the Frequency Domain Decomposition (FDD), as shown in Figure 6, where several peaks below 10 Hz can be considered as resonant frequencies. Again, the traffic noise is clearly visible in the frequency band between 10 and 20 Hz, hiding the resonant peaks at the higher frequencies.

Even if the white noise input assumption is not satisfied, the modal identification of the structure under the traffic loads allows estimating the amplification frequencies due to the structural response (Figure 6). This step is fundamental to quantify the first-mode resonant frequency, allowing a proper selection of the cutting frequency in the high-pass filter for the numerical integration process.

5.2 | Numerical integration

Among all the standards, the Italian code[19] explicitly recommends the direct measurements of the accelerations because of the wide range of frequencies that can be measured (the velocimeters may have some limitations in the measurements of the low frequencies, cutting the major contributions of the structural response). Hence, according to the UNI 9916:2014[19] the time domain integration of the acceleration was performed with the trapezoidal rule after the application of a sixth order Butterworth filter. To minimize the low-frequency drift, the cut-off frequency of the high-pass filter should be carefully selected. The UNI 9916:2014[19] suggests 1 Hz, but also other values can be set to decrease the noise on the obtained values. For instance, in previous work[37] the use of a suitable high-pass IIR or FIR filter without phase distortion is recommended and the cut-off frequency was set equal to 0.001 times the sampling frequency.

Even if the integration in the frequency domain is discouraged by the UNI 9916:2014,[19] the long DFT method seems to be promising to obtain good results with low computational errors.[36] Hence the velocities are herein calculated with both methods, and the results are compared to assess the traffic-induced vibrations. For both methods, the crucial point is the compensation of the low-frequency drift. In the trapezoidal rule a suitable filter should be introduced before the application of the method that is nothing more than a special IIR filter with constant phase equal to 270° and all the poles in the unit circle.[40] In the long DFT method the output signal should be detrended by applying a high-pass filter to obtain the final integrated signals. The filtering frequency cannot be fixed a-priori, because the low-frequency drift depends on several factors (i.e., external noise and electric noise). Thus, a sensitivity analysis was carried out to understand the influence of the selected cut-off frequency on the results obtained with both integration methods. The results are reported in Figure 7 in terms of relative (i) error (δ) between two consecutive cut-off frequencies and (ii) maximum velocities averaged among all the measurement stations ($\overline{v}_{max}$). The cut-off frequencies (f_H) of the sixth order Butterworth filter were normalized with respect to (i) the lower resonant frequency (f_I) and (ii) the sampling rate (f_s).

The results show that both methods stabilize on a decreasing stable-value, suggesting that from the cut-off frequency where the relative error drops down the low-drift components in the signals have been removed. While for the trapezoidal rule the optimal cut-off value can be found at 1.5 Hz, for the DFT this value is increased to 2 Hz. These values correspond respectively to 0.0013 and 0.0017 times the sampling ratio, slightly increasing the values suggested in.[37] Based on the experience on the lodge, it is important to set this limit not so high to avoid the filtering of the contribution of the lowest frequency to the total response. From this perspective the optimal cut-off frequencies correspond to 0.45 and 0.6 times the lowest frequency.

Once the cut-off frequency is selected, a direct comparison of the results obtained with both the numerical integration methods is possible. For instance, the magnitude of the vibrations is very similar giving satisfactory results for both integration methods. As shown in Figure 8 and Figure 9 the integrated signals computed with both methods in the stations at the first level are quite close.

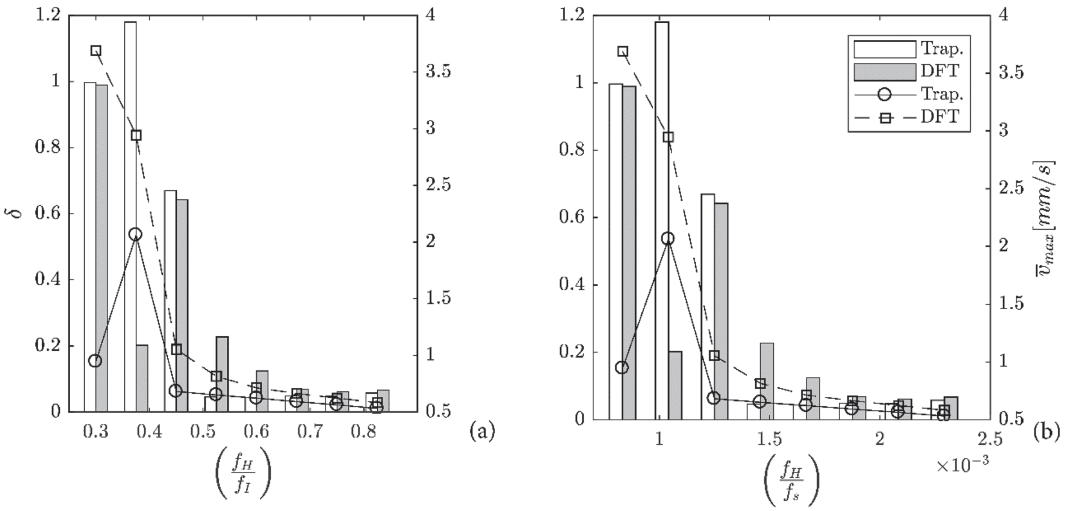

FIGURE 7 Relative error (δ) between two consecutive cut-off frequency of the Hi-pass filter (sixth degree Butterworth) and the obtained maximum velocity averaged among all the signals. The cut-off frequency id represented as a ratio of (a) the lower frequency and (b) the sampling ratio

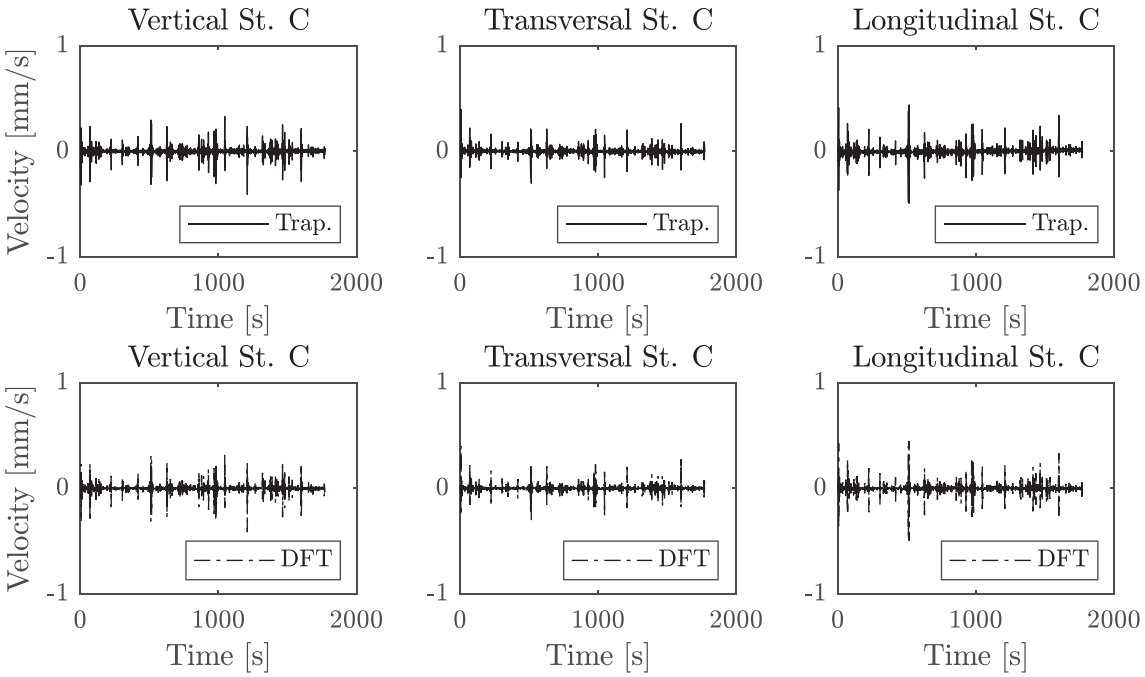

FIGURE 8 The velocities in station C obtained with the trapezoidal rule and the long Discrete Fourier Transform (DFT) method frequency with a high-pass filter equal to 2 Hz

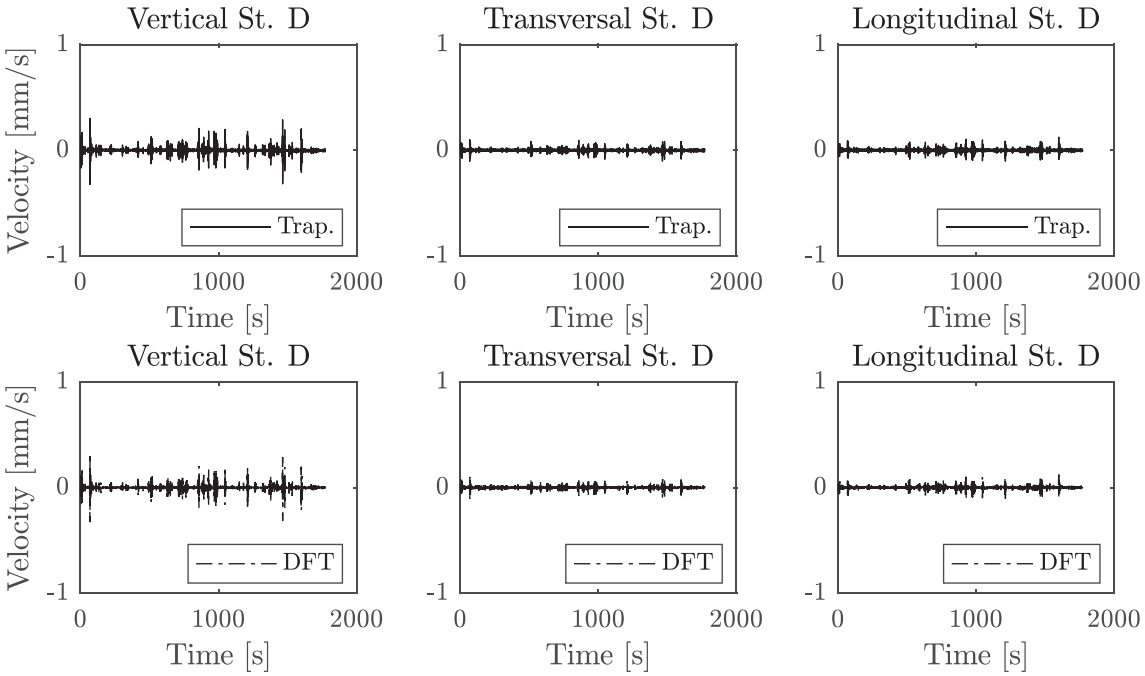

FIGURE 9 The velocities in station D obtained with the trapezoidal rule and the long Discrete Fourier Transform (DFT) method setting the cut-off frequency with a high-pass filter equal to 2 Hz

Concerning the maxima PCPV (Table 4) the results exhibit some slight difference only for the stations at the ground. Thus, the filtering effect of the structure dynamics allows obtaining more reliable results independently from the selected integration method.

TABLE 4 The results of the maximum PCPV for each station calculated with the two integration methods

PCPV [mm/s]						
	Vertical direction		Longitudinal direction		Transversal direction	
Position	*Trap.*	*DFT*	*Trap.*	*DFT*	*Trap.*	*DFT*
A	0.330	0.438	0.192	0.197	0.310	0.430
B	0.179	0.198	0.138	0.251	0.209	0.428
C	0.405	0.414	0.489	0.496	0.395	0.399
D	0.323	0.326	0.123	0.123	0.104	0.105
E	0.372	0.370	0.097	0.098	0.142	0.142

5.3 | Traffic effects

To have an insight on the vibrations induced by the traffic, the event that produces the higher energy was searched in the signals of the February 2019 dynamic testing campaign and its effect on the lodge was analyzed.

A short Fourier transform (SFT) of the velocities was computed for the mean of each component of motion (Figure 10). Thus, the vibrations are mainly characterized by the vertical and longitudinal directions, reaching the highest energy peaks in the frequency band from 8 to 15 Hz confirming the results obtained for the HGV.[39] Each high-energy event corresponds to the single passage of a bus in front of the lodge or, in some cases, the synchronized passage of two buses moving in the opposite directions. The complete timesheet of the buses is reported in the appendix (Table A1).

For instance, the highest energy has been measured in a time window between 900 and 1000 s (Figure 10), corresponding to the passage of two buses in the opposite direction with the start and stop at the bus stop in front of the lodge (Figure 11).

In addition, it is worth noting that in the frequency band between 2.5 and 5 Hz some structural modes can be observed confirming the results of the dynamic identification. As a matter of fact, in this frequency band the energy in the signals is constant for the entire length of the signals.

5.4 | Propagation of the traffic-induced vibration in the lodge

Some additional information about the dynamic interaction of each structural component can be derived from the measurements of the vibrations from the soil to the base of the columns and to the upper part of the lodge. Hence a second layout was adopted in the February 2019 campaign with accelerometers placed along an entire column of the lodge, as shown in Figure 4, in order to analyze the transfer functions for the different traffic sources: both heavy (Figure 12) and light traffic (Figure 13).

Analyzing the vertical components of the records it is possible to observe a significant amplification in the frequency band from 8 to 20 Hz for both heavy and light traffic sources. In the case of heavy-traffic the amplification is clear on such narrow band, while for light traffic some other contributions can be found outside this band. For the components acting in the horizontal plane, amplification can be found for the frequencies below 20 Hz, while a reduction of vibrations can be observed above this frequency. This behavior is more evident in the case of light traffic. Thus, the wider range of frequencies induced by light traffic allows to identify some structural peaks around 5 Hz, confirming again the results of the dynamic identification.

For both traffic sources (heavy and light), it is observed a difference of one order between the spectral amplitudes in the vertical direction and in the horizontal plane. Hence the traffic induced vibrations can be fully characterized. It is observed a prevalence of vertical vibrations in a limited frequency band which is amplified by the structure dynamic response. In addition, only a slight difference between the spectral densities measured by Station C (ground) and by Station B (base of the column) was observed; in fact, the column base and the ground level behave as rigid bodies, while the structural dynamics play an important role, filtering out the high frequency content in the signals.

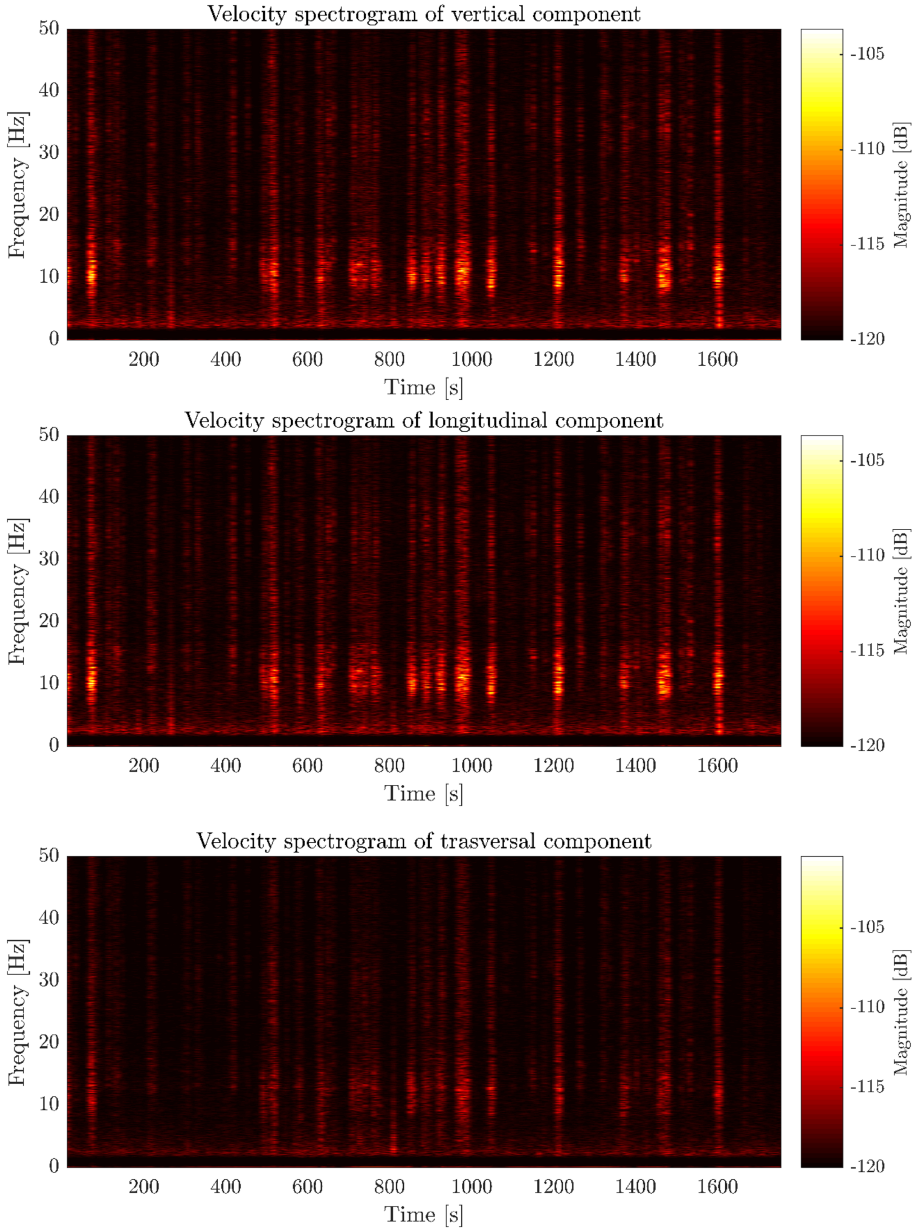

FIGURE 10 The short Fourier transform (SFT) of the velocity for each mean component of motion

5.5 | Propagation of the traffic-induced vibration in the soil

The last step to characterize the traffic-induced vibrations is the analysis of the interaction with the soil and the road pavement. Thus, the experimental campaign performed in June 2019 was employed to characterize the influence of the system pavement-soil in the dynamic response, measured at the ground level. With the FWD machine described in Section 4, several impulsive forces were applied to the pavement in different points of the road and the results are summarized in Figure 14.

The more consistent amplification effects can be observed in station A in the vertical direction, above 100 Hz, while in the structural frequency range (between DC and 50 Hz), an amplification phenomenon can be observed for all the stations at about 35 Hz. This resonance peak is clearly visible for the vertical components, while it is negligible for the horizontal directions (except for the longitudinal component measured in station C).

The spatial distribution of the tests confirms that the amplitude of the resonance peaks increases when the falling weight is closer to the lodge (tests FW-2, FW-3, and FW-5). However, in station B two high peaks at about 150 Hz in the horizontal directions can be observed during the FW-8 test, despite their amplitude is definitively lower during the

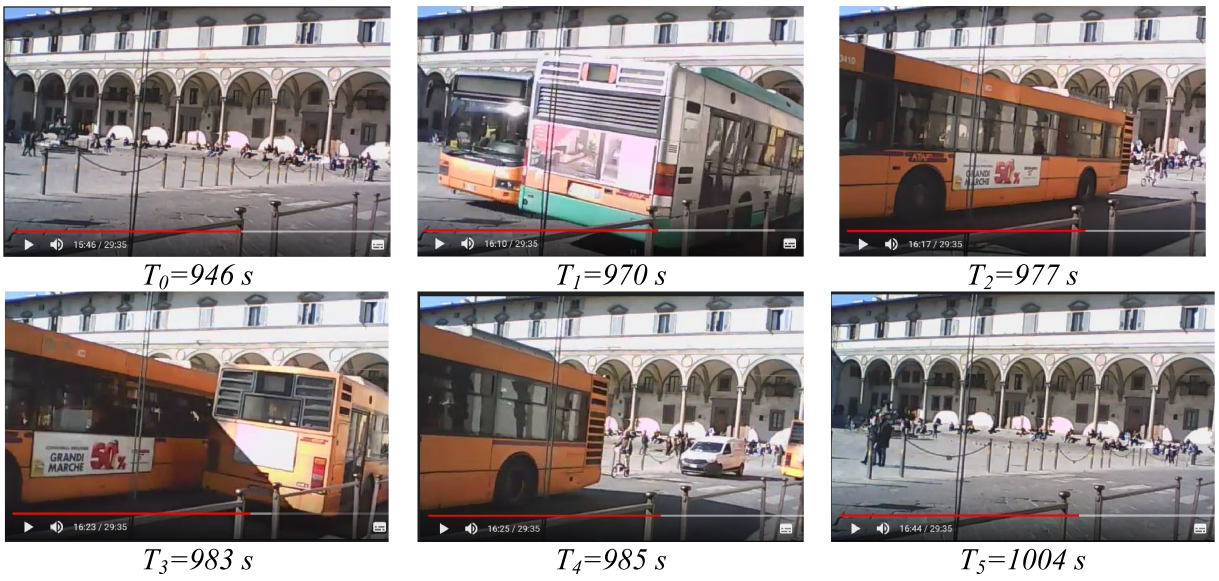

FIGURE 11 The highest-energy event corresponding to a multiple bus-passage in front of the lodge

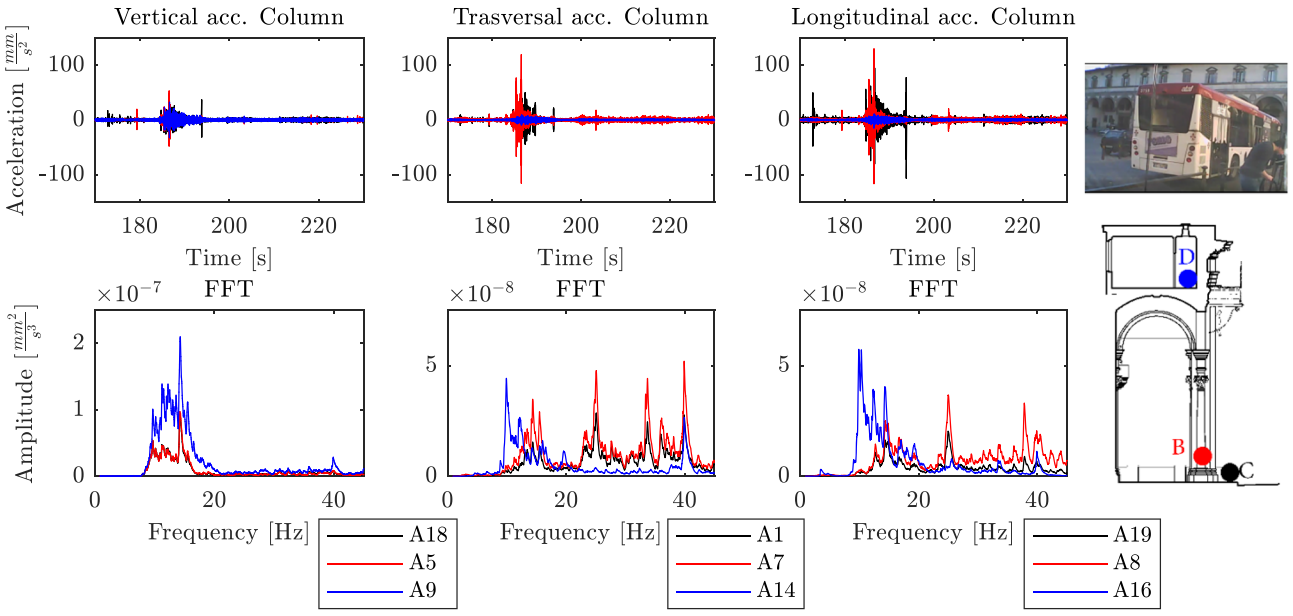

FIGURE 12 The effects of a bus passage measured with the experimental setup #2

FW-3 test. These amplification effects might depend on the local composition of the road pavement nearby the bus stop.

5.6 | Comparison with the 1994 experimental campaign

The February and June 2019 campaigns allowed the evaluation of vibration in the lodge; the PCPV are below both the thresholds proposed by the standards and the values suggested by researchers. Eventually, a comparison with a dynamic testing campaign performed in July 1994 is reported with the aim to check differences in terms of PCPV over these 25 years.

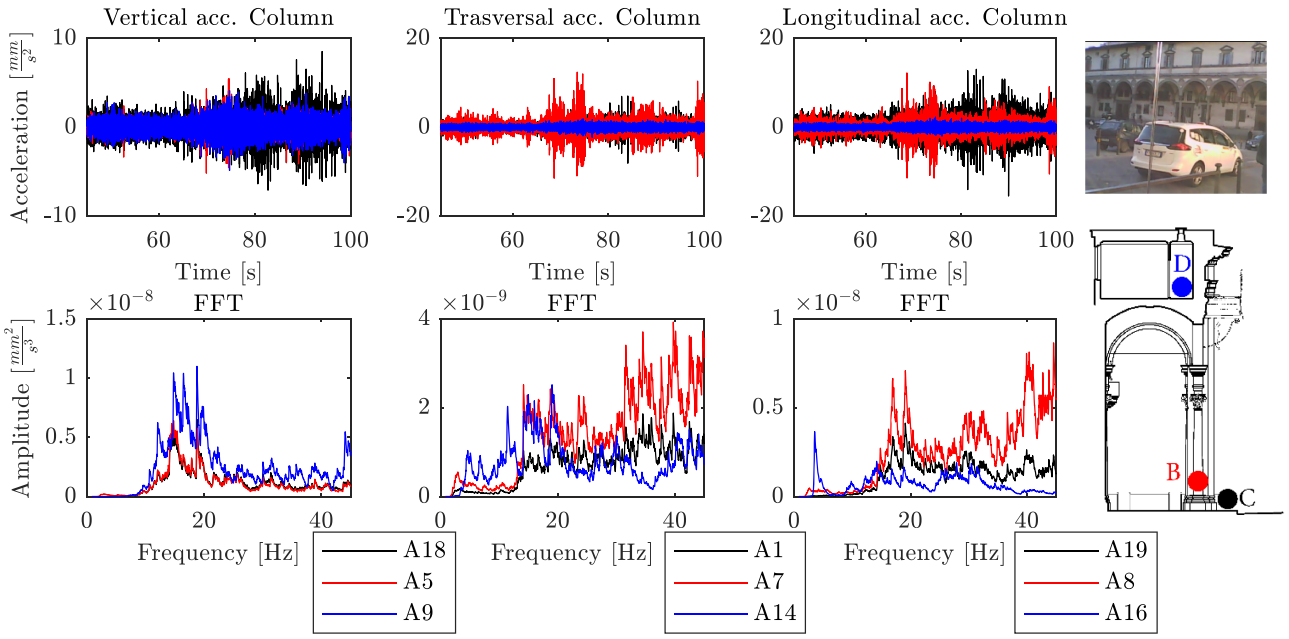

FIGURE 13 The effects of a car passage measured with the experimental setup #2

The 1994 test layout was composed by two measuring stations equipped with inductive accelerometers (HBM B12/200 with a measuring frequency range from 0 to 100 Hz) that correspond to stations B′ and D of the layout reported in Figure 4. The ground level was monitored with accelerometers arranged as a triaxial station, while the first level was monitored only in the vertical and longitudinal direction (i.e. the transversal component was not recorded). The records were sampled at 256 Hz for a length of 120 s corresponding to the passage of a bus. Since no information are available about the bus passages, it is not possible to realize which were the characteristics of the vibration source associated with each signal.

Despite the low sensitivity of the sensors, and the lower sampling frequency, it is possible to compare the results measured at the first level that are filtered by the structure frequency-response function. In this way, the high frequency contribution is reduced and the measured response can be directly compared. In Figure 15 the results of the vertical and longitudinal PCPV, computed using both time and frequency integration methods, are reported setting the same cut-off frequency. In Table 5 the maximum PCPV obtained with the two integration methods are shown for the 1994 testing campaign. A slight difference in the results can be observed: approximatively with a sampling rate six times higher the difference is smaller than 1% (see Table 4) while here it is about 3% measured on the longitudinal component.

Despite the uncertainties connected with an experimental investigation performed about 25 years ago, a general increase of the vibration magnitude can be observed. The values of the PCPV are almost doubled, both in the vertical and longitudinal directions, for the vibration measured at the first level (Station D). Considering that since 1990 the historic city center of Florence is restricted to the traffic, and that the volume of the heavy vehicular traffic may have slightly increased (and that the vibration-source distance is almost the same), a possible cause can be ascribed to the increase of the unevenness in the road pavement (Figure 16).

6 | CONCLUSIVE REMARKS

The traffic-induced vibrations in the old city centers are one of the most important causes for the cosmetic damages in the CH buildings. Even if the phenomenon is well-known and already discussed by the scientific community there is still not a unique framework to assess the acceptable level of vibrations and the National and International Standards establish different limits and procedures.

The paper provides a contribution in this field by analyzing the experimental results on an ancient stone-masonry lodge in Florence prone to traffic-vibrations induced by the heavy-vehicles (buses). Firstly, the methods for the numerical integration of the measured accelerations (PPV or PCPV) were discussed. Provided that a proper calibration of the signals

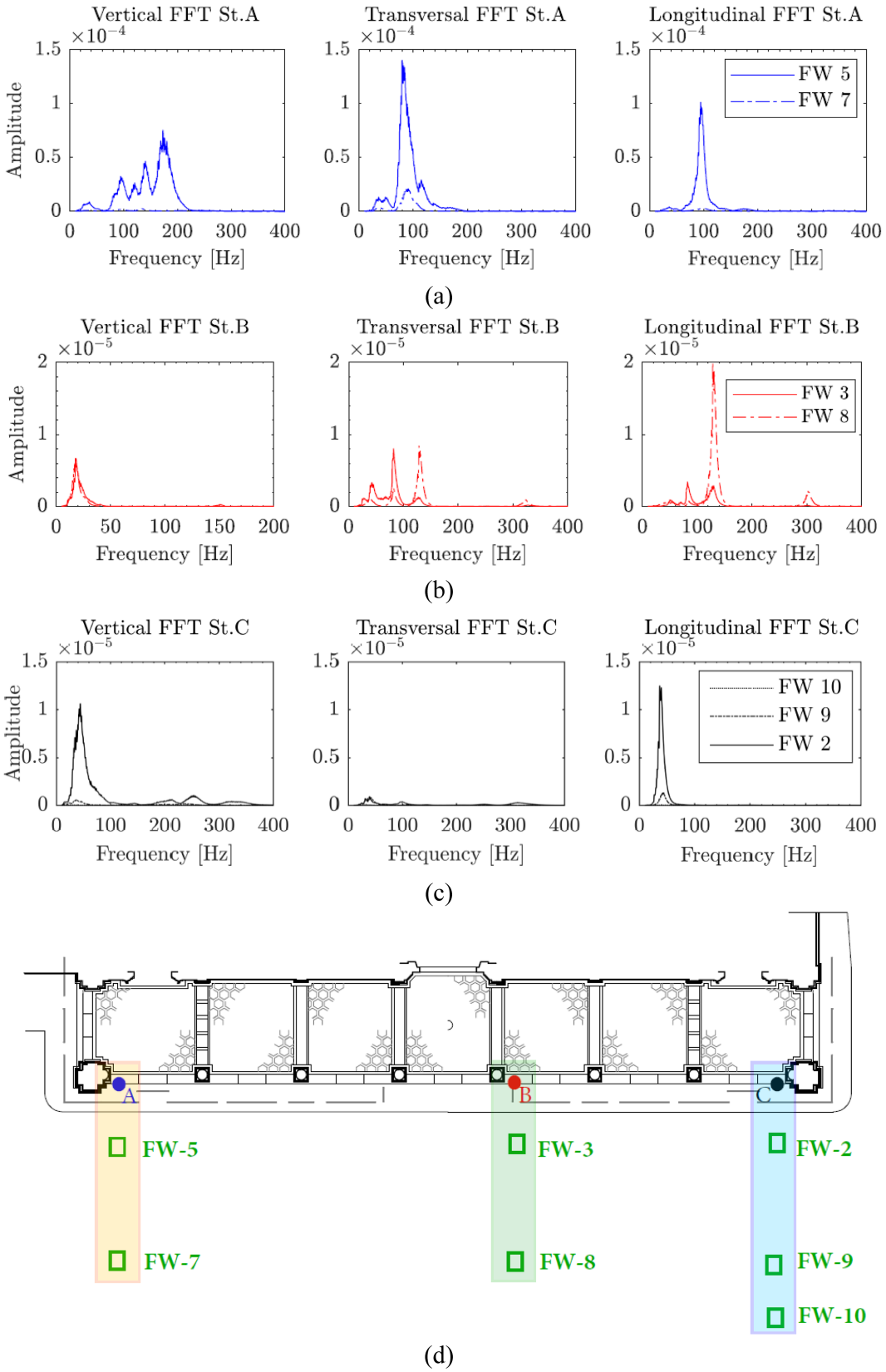

FIGURE 14 (a) Frequency response functions on the alignment A. (b) Frequency Response Functions on the alignment B. (c) Frequency Response Functions on the alignment C. (d) Falling-weight deflectometer (FWD) points

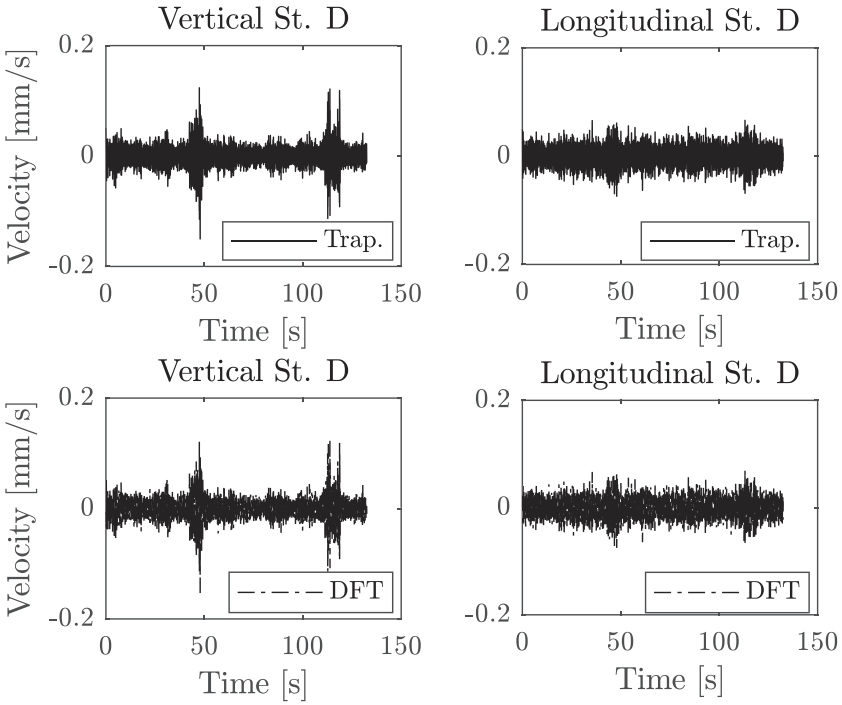

FIGURE 15 The velocities obtained with the direct integration through the trapezoidal rule and the long Discrete Fourier Transform (DFT) methods measured at the first level in the dynamic test campaign of 1994

TABLE 5 The results of the maximum PCPV for the first-floor station calculated with the two integration methods from the signals collected in 1994

PCPV [mm/s]				
	Vertical direction		Longitudinal direction	
Position (Year)	*Trap.*	*DFT*	*Trap.*	*DFT*
D (1994)	0.150	0.153	0.073	0.075
D (2019)	0.323	0.326	0.123	0.123

FIGURE 16 The unevenness in the road surface in front of the measuring stations; (a) Station C, (b) Station B, and (c) Station A

processing method by means of a sensitivity analysis is performed, similar results are obtained with both the trapezoidal rule (operating in the time domain) and the long DFT method (operating in the frequency domain). It was observed that the key-point is the choice of the cut-off frequency in the high-pass filter. As a rule of thumb, to avoid the low-frequency drift phenomenon a value equal to 0.0015 times the sampling frequency is suggested. Moreover, the sampling frequency should be kept as high as possible (at least 1200 Hz) to minimize the numerical errors in the integration process.

Second, the traffic-induced vibrations should be regarded as a continuous source of vibrations that can lead to fatigue phenomena affecting the esthetic parts of the CH buildings (i.e. the plasters, the cornices, and the friezes). The approaches proposed by the Swiss and German standards, based on the engineering judgment, seem to be the most reliable methods. Hence the proposed limits should be carefully considered based on the structure relevance and on the actual cracking pattern.

Lastly, the results of the analyzed case study show that the synchronized passage buses lead to the higher level of vibrations and that the irregularities of the road pavements are one of the most important factors that influences the amplitude. That might explain the increase of the measured vibrations after 25 years from the previous dynamic-test campaign performed in the 1994.

ACKNOWLEDGMENTS

The authors kindly acknowledge the Municipality of Florence for the financial support of this research.

AUTHOR CONTRIBUTIONS

All authors contributed equally to this work. All authors carried out the analyses. The manuscript was written through the contribution of all authors. All authors discussed the results, reviewed, and approved the final version of the manuscript.

DATA AVAILABILITY STATEMENT

Data available on request due to privacy restrictions

ORCID

Giacomo Zini https://orcid.org/0000-0003-3772-2472
Michele Betti https://orcid.org/0000-0002-8389-3355
Gianni Bartoli https://orcid.org/0000-0002-5536-3269

REFERENCES

1. Pau A, Vestroni F. Vibration assessment and structural monitoring of the Basilica of Maxentius in Rome. *Mech Syst Signal Process*. 2013; 41(1-2):454-466. https://doi.org/10.1016/j.ymssp.2013.05.009
2. Baraccani S, Azzara RM, Palermo M, Gasparini G, Trombetti T. Long-term seismometric monitoring of the two towers of bologna (Italy): modal frequencies identification and effects due to traffic induced vibrations, Front. *Built Environ*. 2020;6:1-14. https://doi.org/10.3389/fbuil.2020.00085
3. Crispino M, D'Apuzzo M. Measurement and prediction of traffic-induced vibrations in a heritage building. *J Sound Vib*. 2001;246(2): 319-335. https://doi.org/10.1006/jsvi.2001.3648
4. Clemente P, Rinaldis D. Protection of a monumental building against traffic-induced vibrations. *Soil Dyn. Earthq. Eng.* 1998;17(5): 289-296. https://doi.org/10.1016/S0267-7261(98)00012-8
5. Persson P, Andersen LV, Persson K, Bucinskas P. Effect of structural design on traffic-induced building vibrations. *Procedia Eng*. 2017; 199:2711-2716. https://doi.org/10.1016/j.proeng.2017.09.577
6. Watts GR, Krylov VV. Ground-borne vibration generated by vehicles crossing road humps and speed control cushions. *Appl Acoust*. 2000;59(3):221-236. https://doi.org/10.1016/S0003-682X(99)00026-2
7. Hunt HEM. Modelling of traffic-induced ground vibration as a random process. *J Sound Vib*. 1991;144(1):41-51. https://doi.org/10.1016/0022-460X(91)90731-X
8. Lombaert G, Degrande G. The validation of a numerical prediction model for free field traffic induced vibrations by in situ experiments. *Proc 25th Int Conf Noise Vib Eng ISMA*. 2000;21:379-386.
9. François S, Pyl L, Masoumi HR, Degrande G. The influence of dynamic soil-structure interaction on traffic induced vibrations in buildings. *Soil Dyn. Earthq. Eng.* 2007;27(7):655-674. https://doi.org/10.1016/j.soildyn.2006.11.008
10. Lombaert G, Degrande G, Clouteau D. Numerical modelling of free field traffic-induced vibrations. *Soil Dyn Earthq Eng*. 2000;19(7): 473-488. https://doi.org/10.1016/S0267-7261(00)00024-5
11. Korkmaz KA, Ay Z, Keskin SN, Ceditoglu D. Investigation of traffic-induced vibrations on masonry buildings in turkey and countermeasures, JVC/Journal Vib. *Control*. 2011;17(1):3-10. https://doi.org/10.1177/1077546309346240

12. Monti G, Fumagalli F, Marano GC, Quaranta G, Rea R, Nazzaro B. Effects of ambient vibrations on heritage buildings: overview and wireless dynamic monitoring application. Proc. 3rd Int. Workshop Dynamic Interaction between Soil, Monuments and Built Environment. 2013; 217–229.
13. Hao H, Ang TC, Shen J. Building vibration to traffic-induced ground motion. *Build Environ*. 2001;36(3):321-336. https://doi.org/10.1016/S0360-1323(00)00010-X
14. Tomaževič M, Žnidarič A, Klemenc I, Lavrič I. The influence of traffic induced vibrations on seismic resistance of historic stone masonry buildings, 12th Eur. *Conf Earthq Eng*. 2002;631:1–10.
15. BS 7385-2:1993, Evaluation and measurement for vibration in buildings—part 2: guide to damage levels from groundborne vibration, British Standards Institution. 1993.
16. DIN 4150-3:1999, Structural vibrations—part 3: effects of vibration on structures, Deutsches Institut fur Normung. 2016.
17. ISO, 4866:2010, Mechanical vibration and shock—vibration of fixed structures—guidelines for the measurement of vibrations and evaluation of their effects on structures, International Organization for Standardization. 2010.
18. SN 640312:2013, Effet des ébranlements sur les constructions, Swiss Standard. 2013.
19. UNI 9916:2014, Criteri di misura e valutazione degli effetti delle vibrazioni sugli edifici, Ente Nazionale Italiano di Unificazione. 2014.
20. Ainalis D, Ducarne L, Kaufmann O, Tshibangu JP, Verlinden O, Kouroussis G. Improved analysis of ground vibrations produced by man-made sources. *Sci Total Environ*. 2018;616–617:517-530. https://doi.org/10.1016/j.scitotenv.2017.10.291
21. Lak MA, Degrande G, Lombaert G. The effect of road unevenness on the dynamic vehicle response and ground-borne vibrations due to road traffic. *Soil Dyn. Earthq. Eng.* 2011;31(10):1357-1377. https://doi.org/10.1016/j.soildyn.2011.04.009
22. Pieraccini M. Extensive measurement campaign using interferometric radar. *J Perform Constr Facil*. 2017;31(3):04016113. https://doi.org/10.1061/(ASCE)CF.1943-5509.0000987
23. Pieraccini M, Betti M, Forcellini D, et al. Radar detection of pedestrian-induced vibrations on Michelangelo's David. *PLoS One*. 2017;12(4):1-20. https://doi.org/10.1371/journal.pone.0174480
24. Pallarés FJ, Betti M, Bartoli G, Pallarés L. Structural health monitoring (SHM) and Nondestructive testing (NDT) of slender masonry structures: a practical review. *Construct Build Mater*. 2021;279:123768. https://doi.org/10.1016/j.conbuildmat.2021.123768
25. Konon W, Schuring JR. Vibration criteria for historic buildings. *J Constr Eng and Manag*. 1985;111(3):208-215. https://doi.org/10.1061/(ASCE)0733-9364(1985)111:3(208)
26. Transportation and construction vibration guidance manual, California Department of Transportation, (2013).
27. Domenichini L, Crispino M, D'apuzzo M, Ferro R. Road traffic induced noise and vibration. *Proc XXIII PIARC Road National Conference*. 1998;69-118.
28. Roselli I, Fioriti V, Bellagamba I, et al. De Canio, Impact of traffic vibration on the temple of Minerva Medica, Rome: preliminary study within the co.b.ra. project. *Int J Herit Archit Stud Repairs Maintence*. 2017;2(1):102-114. https://doi.org/10.2495/ha-v2-n1-102-114
29. Erkal A. Transmission of traffic-induced vibrations on and around the Minaret of Little Hagia Sophia. *Int J Archit Herit*. 2017;11:349-362. https://doi.org/10.1080/15583058.2016.1230657
30. Ma M, Markine V, Liu WN, Yuan Y, Zhang F. Metro train-induced vibrations on historic buildings in Chengdu, China. *J Zhejiang Univ Sci a*. 2011;12(10):782-793. https://doi.org/10.1631/jzus.A1100088
31. Fratini M, Pieraccini M, Atzeni C, Betti M, Bartoli G. Assessment of vibration reduction on the Baptistery of San Giovanni in Florence (Italy) after vehicular traffic block. *J Cult Herit*. 2011;12(3):323-328. https://doi.org/10.1016/j.culher.2011.01.003
32. Pau A, Vestroni F. Vibration analysis and dynamic characterization of the Colosseum. *Struct Control Heal Monit*. 2008;15(8):1105-1121. https://doi.org/10.1002/stc.253
33. Kliukas R, Jaras A, Kačianauskas R. Investigation of traffic-induced vibration in vilnius arch-cathedral belfry. *Transport*. 2008;23(4):323-329. https://doi.org/10.3846/1648-4142.2008.23.323-329
34. Clemente P. Traffic-induced vibrations on structures. *IABSE Report*. 73(2):1111-1116. https://doi.org/10.5169/seals-55319
35. Chiostrini S, Marradi A, Vignoli A. *Evaluation of traffic-induced vibrations in historic buildings: the case of the "Galleria Vasariana" in Florence*. WIT Press; 1995:17 doi: 10.2495/STR950092.
36. Brandt A, Brincker R. Integrating time signals in frequency domain—comparison with time domain integration. *Meas J Int Meas Confed*. 2014;58:511-519. https://doi.org/10.1016/j.measurement.2014.09.004
37. Brandt A. *Noise and Vibration Analysis: Signal Analysis and Experimental Procedures*. 2011:1-438. https://doi.org/10.1002/9780470978160
38. Pratelli C, Betti G, Giuffrè T, Marradi A. Preliminary in-situ evaluation of an innovative, semi-flexible pavement wearing course mixture using Fast Falling Weight Deflectometer. *Materials*. 2018;11(4):1-14. https://doi.org/10.3390/ma11040611
39. Watts GR. The generation and propagation of vibration in various soils produced by the dynamic loading of road pavements. *J Sound Vib*. 1992;156(2):191-206. https://doi.org/10.1016/0022-460X(92)90692-Q
40. Pintelon R, Schoukens J. Real-time integration and differentiation of analog signals by means of digital filtering. *IEEE Trans on Instr and Measur*. 1990;39:346-352. https://doi.org/10.1109/imtc.1990.66036

How to cite this article: Zini G, Betti M, Bartoli G. Experimental analysis of the traffic-induced-vibration on an ancient lodge. *Struct Control Health Monit*. 2022;29(3):e2900. doi:10.1002/stc.2900

APPENDIX A: BUS PASSAGES IN FRONT OF THE LODGE

TABLE A1 Vehicle passage in the measurement presented herein

Vehicle	Time [s]	Direction
Two buses	5	COL/SM
Bus	69	SM
Bus	496	COL
Bus	511	SM
Bus	585	COL
Bus	628	SM
Bus	712	COL
Bus	729	COL
Bus	764	SM
Bus	852	COL
Bus	888	COL
Bus	923	COL
Two buses	970	COL/SM
Two buses	984	COL/SM
Bus	1045	SM
Bus	1209	SM
Bus	1330	COL
Bus	1461	COL
Bus	1475	COL
Bus	1599	SM
Truck	1670	COL

Note: The direction COL means to Via la Colonna and SM to Piazza San Marco (see Figure A1).

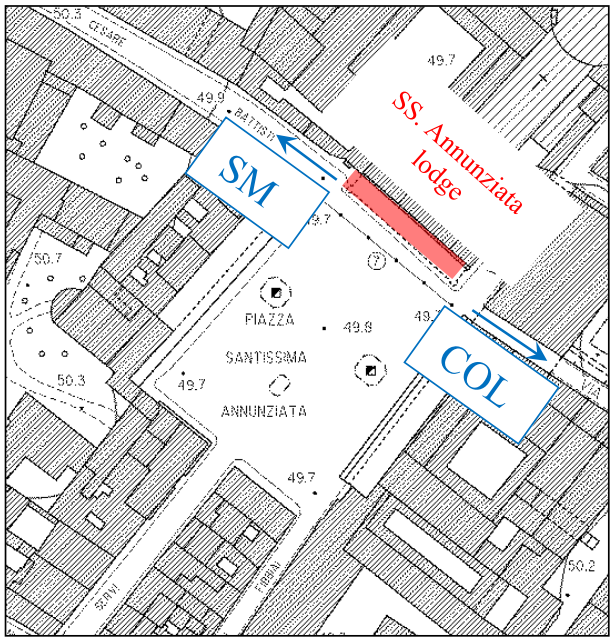

FIGURE A1 Plan of the SS Annunziata square: In red the lodge and the vehicular-traffic main direction (SM to Piazza San Marco, and COL to via della Colonna)